Collective phenomena and shell structure far from stability

Frédéric Nowacki[1]

NUCLEAR PHYSICS AT THE EDGE
OF STABILITY

04 July 2022 — 08 July 2022 Hybrid/Mixed

CNRS IN2P3 Les deux infinis — IPHC Institut Pluridisciplinaire Hubert Curien Strasbourg — Université de Strasbourg

[1] Strasbourg-Madrid Shell-Model collaboration

Landscape of medium mass nuclei

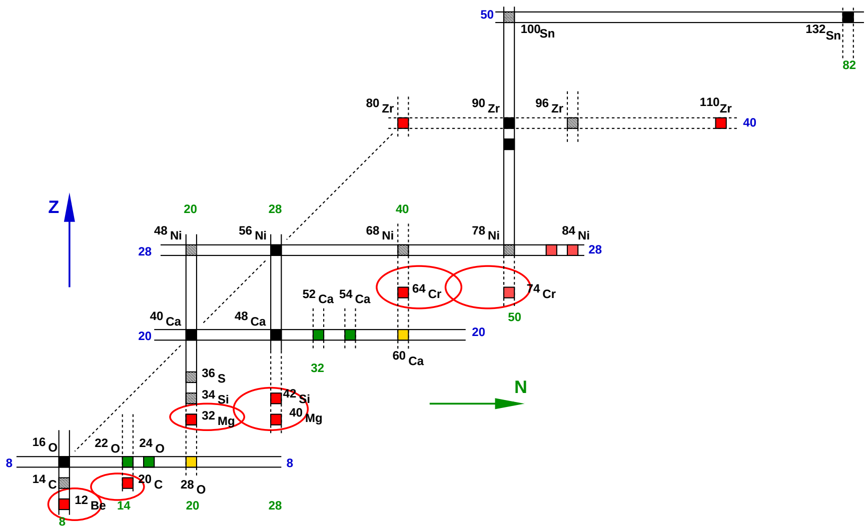

Landscape of medium mass nuclei

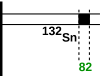

Z

- New gaps: ^{24}O, ^{48}Ni, ^{54}Ca, ^{78}Ni, ^{100}Sn
- Vanishing of shell closure: ^{12}Be, ^{32}Mg, ^{42}Si, ^{64}Cr, ^{80}Zr ...
- Island of deformation around A$\sim$ 32, A$\sim$ 64
- Low-lying dipole excitations in Ne, Ni isotopes

- Variety of phenomena dictated by shell structure
- Close connection between collective behaviour and underlying shell structure
- Interplay between
  - Monopole field (spherical mean field)
  - Multipole correlations (pairing, Q.Q, ...)

"Pairing plus Quadrupole propose, Monopole disposes"
A. Zuker, Coherent and Random Hamiltonians, CRN Preprint 1994

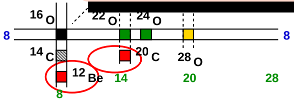

Development of deformation at N=8,20,40,70

^{12}Be π ν π ν ^{32}Mg

- Magic numbers are associated to enegy gaps in the spherical mean field. Therefore, to promote particles above the Fermi levels costs energy
- However some intruders configurations can overwhelm their loss of monopole energy with their huge gain in correlation energy
- Several examples of this phenomenon exist in stable magic nuclei (as in ^{40}Ca nucleus) in the form of coexisting spherical, deformed and superdeformed states in a very narrow energy range
- At the very neutron rich or very proton rich edges, the T=0 and T=1 channels of the effective nuclear interaction weight very differently than they do at the stability line. Therefore the effective single particle structure may suffer important changes, leading in some cases to the vanishing of established shell closures or to the appearance of new ones

^{64}Cr N=3 N=4 ^{14}Ru

Development of deformation at N=8,20,40,70

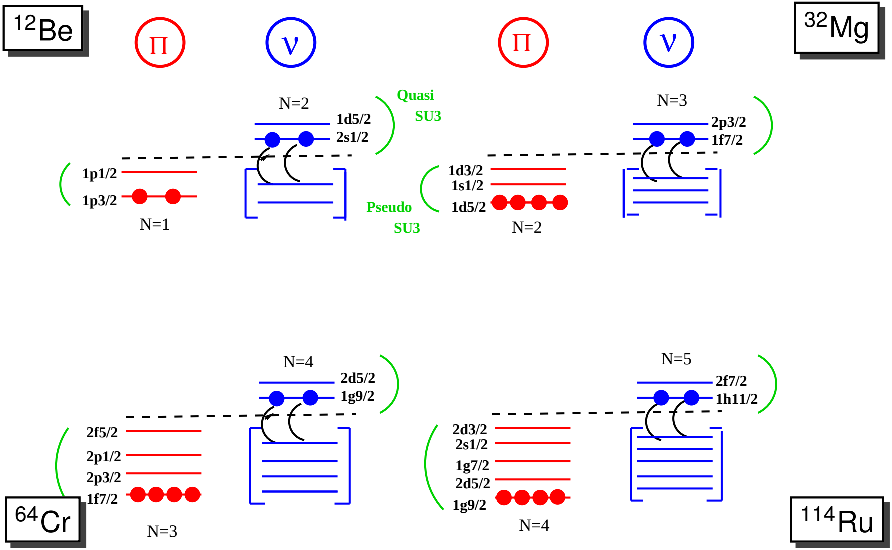

Shell Model: Physics Goals

Collective excitations:

- Deformation, Superdeformation,

Dipole/M1 resonances

- Superfluidity
- Symmetries

Weak processes:

- β decay
- $\beta\beta$ decay

$$[T^{0\nu}_{1/2}(0^+ \to 0^+)]^{-1} = G_{0\nu}|M^{0\nu}|^2\langle m_\nu\rangle^2$$

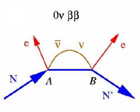

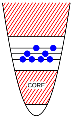

- define Effective Interaction
- $\mathcal{H}_{\rm eff}\Psi_{\rm eff} = E\Psi_{\rm eff}$
- build and diagonalize Energy matrix

Shell evolution far from stability:

- Vanishing of shell closures
- New magic numbers

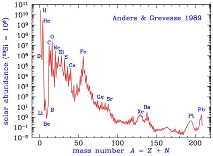

Ab Initio calculations:

- Chiral EFT realistic interactions
- 3N forces

Shell Model: Giant Computations

- exponential growth of basis dimensions:

$$D \sim \binom{d_\pi}{p} \cdot \binom{d_\nu}{n}$$

In *pf* shell :

^{48}Cr	1,963,461
^{56}Ni	**1,087,455,228**

In *pf-sdg* space :

^{78}Ni	**210,046,691,518**

- Actual limits in limits in giant diagonalizations: **0.2 10^{12}** for ^{114}Sn core excitations

- Some of the largest diagonalizations ever are performed in Strasbourg with relatively modest computationnal ressources:
  Phys. Rev. C82 (2010) 054301, ibidem 064304

  - m scheme — ANTOINE code
  - coupled scheme — NATHAN code

E. Caurier et al., Rev. Mod. Phys. 77 (2005) 427; ANTOINE website

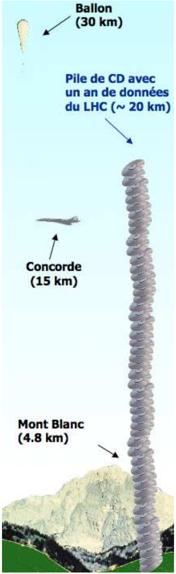

- Largest matrices up to now contain up to ~ **10^{14}** non-zero matrix elements.

- This would require more than 1,000,000 CD-ROM's to store the information for a single matrix !

- They cannot be stored on hard disk and are computed on the fly.

Shell Model: Giant Computations

- exponential growth of basis dimensions:

$$D \sim \begin{pmatrix} d_\pi \\ p \end{pmatrix} \cdot \begin{pmatrix} d_\nu \\ n \end{pmatrix}$$

In *pf* shell :

^{48}Cr 1,963,461

^{56}Ni **1,087,455,228**

In *pf-sdg* space :

^{78}Ni **210,046,691,518**

- Actual limits in limits in giant diagonalizations: **0.2 10^{12}** for ^{114}Sn core excitations

- Some of the largest diagonalizations ever are performed in Strasbourg with relatively modest computationnal ressources:
Phys. Rev. C82 (2010) 054301, ibidem 064304

  - m scheme ANTOINE code
  - coupled scheme NATHAN code

E. Caurier et al., Rev. Mod. Phys. 77 (2005) 427; ANTOINE website

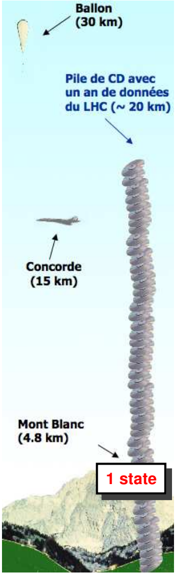

- Largest matrices up to now contain up to **$\sim 10^{14}$** non-zero matrix elements.

- This would require more than 1,000,000 CD-ROM's to store the information for a single matrix !

- They cannot be stored on hard disk and are computed on the fly.

Shell Model: Giant Computations

- exponential growth of basis dimensions:

$$D \sim \begin{pmatrix} d_\pi \\ p \end{pmatrix} \cdot \begin{pmatrix} d_\nu \\ n \end{pmatrix}$$

In *pf* shell :
^{48}Cr 1,963,461
^{56}Ni **1,087,455,228**
In *pf-sdg* space :
^{78}Ni **210,046,691,518**

- Actual limits in limits in giant diagonalizations: **0.2 10^{12}** for ^{114}Sn core excitations

- Some of the largest diagonalizations ever are performed in Strasbourg with relatively modest computationnal ressources:
Phys. Rev. C82 (2010) 054301, ibidem 064304

- m scheme ANTOINE code
- coupled scheme NATHAN code

E. Caurier et al., Rev. Mod. Phys. 77 (2005) 427; ANTOINE website

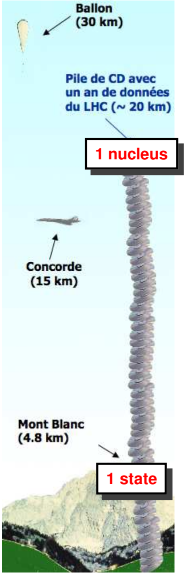

- Largest matrices up to now contain up to ∼ **10^{14}** non-zero matrix elements.

- This would require more than 1,000,000 CD-ROM's to store the information for a single matrix !

- They cannot be stored on hard disk and are computed on the fly.

Shell Model: Giant Computations

- exponential growth of basis dimensions:

$$D \sim \begin{pmatrix} d_\pi \\ p \end{pmatrix} \cdot \begin{pmatrix} d_\nu \\ n \end{pmatrix}$$

In *pf* shell :

^{48}Cr   1,963,461

^{56}Ni   **1,087,455,228**

In *pf-sdg* space :

^{78}Ni   **210,046,691,518**

- Actual limits in limits in giant diagonalizations: **0.2 10^{12}** for ^{114}Sn core excitations
- Some of the largest diagonalizations ever are performed in Strasbourg with relatively modest computationnal ressources:

Phys. Rev. C82 (2010) 054301, ibidem 064304

- m scheme   ANTOINE code
- coupled scheme   NATHAN code

E. Caurier et al., Rev. Mod. Phys. 77 (2005) 427; ANTOINE website

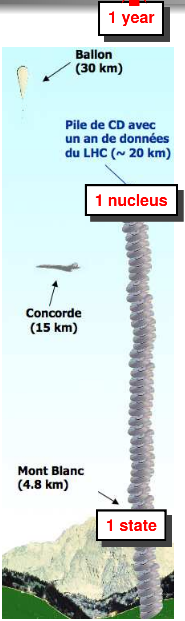

- Largest matrices up to now contain up to $\sim$ **10^{14}** non-zero matrix elements.
- This would require more than 1,000,000 CD-ROM's to store the information for a single matrix !
- They cannot be stored on hard disk and are computed on the fly.

Shell Model: Giant Computations

PHYSICAL REVIEW C **105**, 054314 (2022)

Nuclear structure within a discrete nonorthogonal shell model approach: New frontiers

D. D. Dao and F. Nowacki
Université de Strasbourg, CNRS, IPHC UMR7178, 23 rue du Loess, F-67000 Strasbourg, France

(Received 8 March 2022; accepted 6 May 2022; published 23 May 2022)

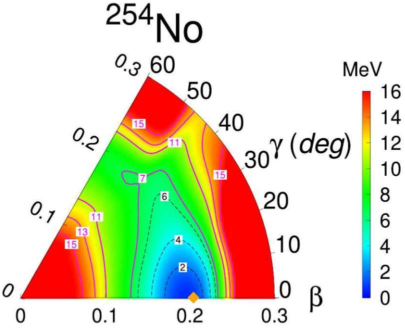

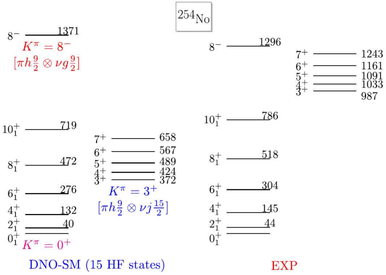

First “SM” calculations for superheavies !!!

The nuclear interaction: the complex view

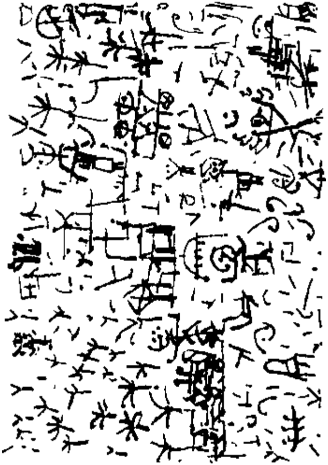

P. Klee, art

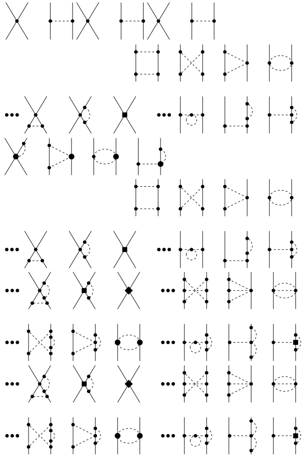

E. Epelbaum, physics

The nuclear interaction: the simple view

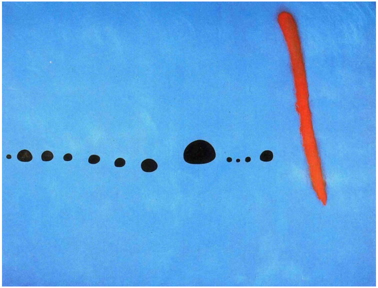

J. Miro, art

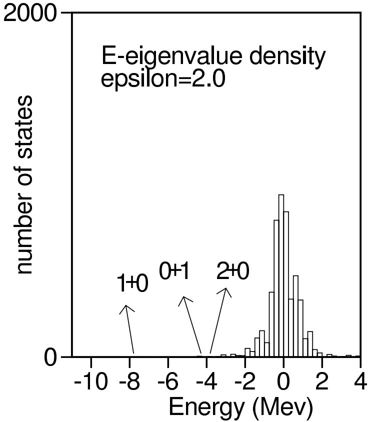

A. Zuker, physics

Separation of the effective Hamiltonian
Monopole and multipole

From the work of M. Dufour and A. Zuker (PRC 54 1996 1641)
Separation theorem:

Any effective interaction can be split in two parts:

$$H = H_{monopole} + H_{multipole}$$

$H_{monopole}$: *spherical mean-field*
☞responsible for the global saturation properties and for the evolution of the spherical single particle levels.
$H_{multipole}$: *correlator*
☞ pairing, quadrupole, octupole...

Important property:

$$\langle CS \pm 1|H|CS \pm 1\rangle = \langle CS \pm 1|H_{monopole}|CS \pm 1\rangle$$

Multipole Hamiltonian

$H_{multipole}$ can be written in two representations, particle-particle and particle-hole. Both can be brought into a diagonal form. When this is done, it comes out that only a few terms are coherent, and those are the simplest ones:

- $L = 0$ isovector and isoscalar pairing
- Elliott's quadrupole
- $\vec{\sigma}\vec{\tau} \cdot \vec{\sigma}\vec{\tau}$
- Octupole and hexadecapole terms of the type $r^\lambda Y_\lambda \cdot r^\lambda Y_\lambda$

Besides, they are universal (all the realistic interactions give similar values) and scale simply with the mass number

	pp(JT)			ph($\lambda\tau$)			
	10	01	21	20	40	10	11
KB	-5.83	-4.96	-3.21	-3.53	-1.38	+1.61	+3.00
USD-A	-5.62	-5.50	-3.17	-3.24	-1.60	+1.56	+2.99
CCEI	-6.79	-4.68	-2.93	-3.40	-1.39	+1.21	+2.83
NN+NNN-MBPT	-6.40	-4.36	-2.91	-3.28	-1.23	+1.10	+2.43
NN-MBPT	-6.06	-4.38	-2.92	-3.35	-1.31	+1.03	+2.49

Multipole Hamiltonian

$H_{multipole}$ can be written in two representations, particle-particle
and pa
When
cohere

- L =
- Ell
- $\vec{\sigma}\vec{\tau}$
- Oc

Beside
similar

KB	0
USD	9
CCE	8
NN+	8
NN-	9

- **Pairing regime: spherical nuclei**
  ground state = pairs of like-particles coupled at J=0 (seniority v=0)
  2^+ state (break of pair; v=2) at high energy

  superfluid nucleus:

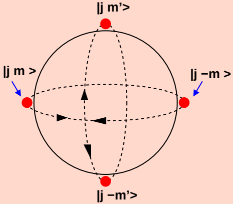

Typical example: **Tin isotopes**

- **Quadrupole regime: deformed nuclei**

  prolate nucleus:

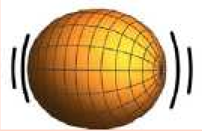

Typical example: **open shell N=Z nuclei**

Multipole Hamiltonian

$H_{multipole}$ can be written in two representations, particle-particle and particle-hole. Both can be brought into a diagonal form. When this is done, it comes out that only a few terms are coherent, and those are the simplest ones:

- $L = 0$ isovector and isoscalar pairing
- Elliott's quadrupole
- $\vec{\sigma}\vec{\tau} \cdot \vec{\sigma}\vec{\tau}$
- Octupole and hexadecapole terms of the type $r^\lambda Y_\lambda \cdot r^\lambda Y_\lambda$

Besides, they are universal (all the realistic interactions give similar values) and scale simply with the mass number

	pp(JT)			ph($\lambda\tau$)			
	10	01	21	20	40	10	11
KB	-5.83	-4.96	-3.21	-3.53	-1.38	+1.61	+3.00
USD-A	-5.62	-5.50	-3.17	-3.24	-1.60	+1.56	+2.99
CCEI	-6.79	-4.68	-2.93	-3.40	-1.39	+1.21	+2.83
NN+NNN-MBPT	-6.40	-4.36	-2.91	-3.28	-1.23	+1.10	+2.43
NN-MBPT	-6.06	-4.38	-2.92	-3.35	-1.31	+1.03	+2.49

Multipole Hamiltonian

$H_{multipole}$ can be written in two representations, particle-particle and particle-hole. Both can be brought into a diagonal form. When this is done, it comes out that only a few terms are coherent, and those are the simplest ones:

- $L = 0$ isovector and isoscalar pairing
- Elliott's quadrupole
- $\vec{\sigma}\vec{\tau} \cdot \vec{\sigma}\vec{\tau}$
- Octupole and hexadecapole terms of the type $r^\lambda Y_\lambda \cdot r^\lambda Y_\lambda$

Besides, they are universal (all the realistic interactions give similar values) and scale simply with the mass number

	pp(JT)		ph(λτ)				
	10	01	21	20	40	10	11
KB	-5.83	-4.96	3.21	-3.53	-1.38	+1.61	+3.00
USD-A	-5.62	-5.50	3.17	-3.24	-1.60	+1.56	+2.99
CCEI	-6.79	-4.68	2.93	-3.40	-1.39	+1.21	+2.83
NN+NNN-MBPT	-6.40	-4.36	2.91	-3.28	-1.23	+1.10	+2.43
NN-MBPT	-6.06	-4.38	2.92	-3.35	-1.31	+1.03	+2.49

Multipole Hamiltonian

$H_{multipole}$ can be written in two representations, particle-particle and particle-hole. Both can be brought into a diagonal form. When this is done, it comes out that only a few terms are coherent, and those are the simplest ones:

- $L = 0$ isovector and isoscalar pairing
- Elliott's quadrupole
- $\vec{\sigma}\vec{\tau} \cdot \vec{\sigma}\vec{\tau}$
- Octupole and hexadecapole terms of the type $r^\lambda Y_\lambda \cdot r^\lambda Y_\lambda$

Besides, they are universal (all the realistic interactions give similar values) and scale simply with the mass number

	pp(JT)				ph($\lambda\tau$)		
	10	01	21	20	40	10	11
KB	-5.83	-4.96	-3.21	-3.53	-1.38	+1.61	+3.00
USD-A	-5.62	-5.50	-3.17	-3.24	-1.60	+1.56	+2.99
CCEI	-6.79	-4.68	-2.93	-3.40	-1.39	+1.21	+2.83
NN+NNN-MBPT	-6.40	-4.36	-2.91	-3.28	-1.23	+1.10	+2.43
NN-MBPT	-6.06	-4.38	-2.92	-3.35	-1.31	+1.03	+2.49

Multipole Hamiltonian

$H_{multipole}$ can be written in two representations, particle-particle and particle-hole. Both can be brought into a diagonal form. When this is done, it comes out that only a few terms are coherent, and those are the simplest ones:

- $L = 0$ isovector and isoscalar pairing
- Elliott's quadrupole
- $\vec{\sigma}\vec{\tau} \cdot \vec{\sigma}\vec{\tau}$
- Octupole and hexadecapole terms of the type $r^\lambda Y_\lambda \cdot r^\lambda Y_\lambda$

Besides, they are universal (even from modern abinitio derivations, all the realistic interactions give similar values) and scale simply with the mass number

particle-particle		Interaction	particle-hole		
$JT = 01$	$JT = 10$		$\lambda\tau = 20$	$\lambda\tau = 40$	$\lambda\tau = 11$
-5.42	-5.43	KLS	-2.90	-1.61	+2.38
-5.48	-6.24	BONNB	-2.82	-1.39	+3.64
-5.69	-5.90	USD	-3.18	-1.60	+3.08
-4.75	-4.46	KB3	-2.79	-1.39	+2.46
-5.06	-5.08	FPD6	-3.11	-1.67	+3.17
-4.07	-5.74	GOGNY	-3.23	-1.77	+2.46

Multipole Hamiltonian

$H_{multipole}$ can be written in two representations, particle-particle and particle-hole. Both can be brought into a diagonal form. When this is done, it comes out that only a few terms are coherent, and those are the simplest ones:

- $L = 0$ isovector and isoscalar pairing
- Elliott's quadrupole
- $\vec{\sigma}\vec{\tau} \cdot \vec{\sigma}\vec{\tau}$
- Octupole and hexadecapole terms of the type $r^{\lambda} Y_{\lambda} \cdot r^{\lambda} Y_{\lambda}$

Besides, they are universal (even from modern abinitio derivations, all the realistic interactions give similar values) and scale simply with the mass number

particle-particle		Interaction	particle-hole		
$JT = 01$	$JT = 10$		$\lambda\tau = 20$	$\lambda\tau = 40$	$\lambda\tau = 11$
-5.42	-5.43	KLS	-2.90	-1.61	+2.38
-5.48	-6.24	BONNB	-2.82	-1.39	+3.64
-5.69	-5.90	USD	-3.18	-1.60	+3.08
-4.75	-4.46	KB3	-2.79	-1.39	+2.46
-5.06	-5.08	FPD6	-3.11	-1.67	+3.17
-4.07	-5.74	GOGNY	-3.23	-1.77	+2.46

Multipole Hamiltonian

$H_{multipole}$ can be written in two representations, particle-particle and particle-hole. Both can be brought into a diagonal form. When this is done, it comes out that only a few terms are coherent, and those are the simplest ones:

- $L = 0$ isovector and isoscalar pairing
- Elliott's quadrupole
- $\vec{\sigma}\vec{\tau} \cdot \vec{\sigma}\vec{\tau}$
- Octupole and hexadecapole terms of the type $r^{\lambda} Y_{\lambda} \cdot r^{\lambda} Y_{\lambda}$

Besides, they are universal (even from modern abinitio derivations, all the realistic interactions give similar values) and scale simply with the mass number

particle-particle		Interaction	particle-hole		
$JT = 01$	$JT = 10$		$\lambda\tau = 20$	$\lambda\tau = 40$	$\lambda\tau = 11$
-5.42	-5.43	KLS	-2.90	-1.61	+2.38
-5.48	-6.24	BONNB	-2.82	-1.39	+3.64
-5.69	-5.90	USD	-3.18	-1.60	+3.08
-4.75	-4.46	KB3	-2.79	-1.39	+2.46
-5.06	-5.08	FPD6	-3.11	-1.67	+3.17
-4.07	-5.74	GOGNY	-3.23	-1.77	+2.46

Playground

In the valence space of two major shells

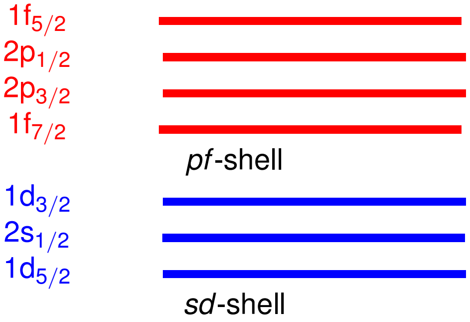

EFFECTIVE INTERACTION: SDPF-U-MIX (update 2020)

Island of Inversion: Trends

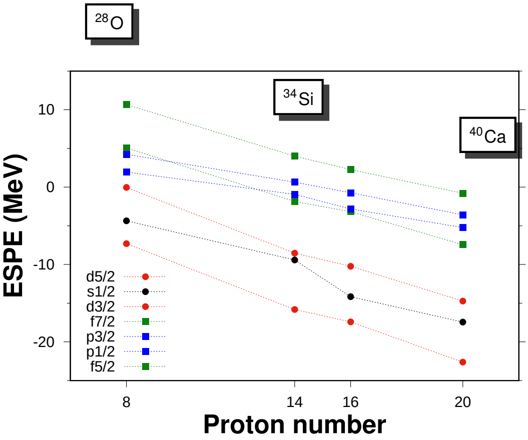

- At the neutron drip line, the ESPE's of ^{28}O are completely at variance with those of ^{40}Ca at the stability valley. The change from the standard ESPE's of ^{16}O to the anomalous ones in ^{28}O is totally due to the interactions of *sd* shell neutrons among themselves
- Notice that the *sd* shell orbits remain always below th *pf* shell with the $\nu 0 f_{\frac{7}{2}}$ and $\nu 0 p_{\frac{3}{2}}$ orbitals DO get inverted
- The monopole part of the neutron-proton interaction restores the N=20 shell gap when the valley of stability is approached
- Spin-Tensor decomposition shows it is mainly a Central and Tensor effect

Islands Of Inversion: Trends

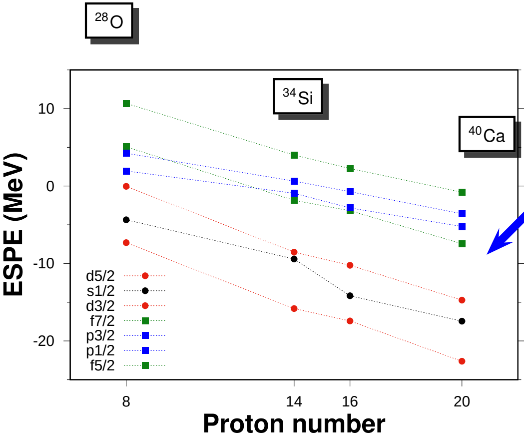

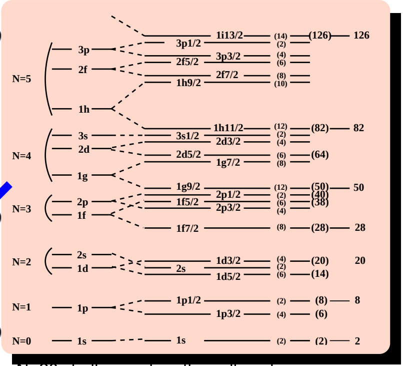

- N=20 shell gap when the valley of stability is approached
- Spin-Tensor decomposition shows it is mainly a Central and Tensor effect

Island of Inversion: Trends

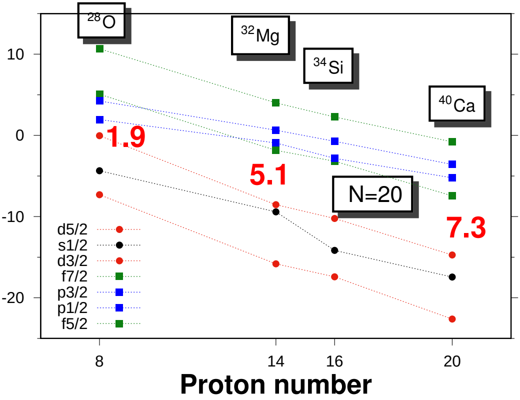

- At the neutron drip line, the ESPE's of ^{28}O are completely at variance with those of ^{40}Ca at the stability valley. The change from the standard ESPE's of ^{16}O to the anomalous ones in ^{28}O is totally due to the interactions of *sd* shell neutrons among themselves
- Notice that the *sd* shell orbits remain always below th *pf* shell with the $\nu 0f_{\frac{7}{2}}$ and $\nu 0p_{\frac{3}{2}}$ orbitals DO get inverted
- The monopole part of the neutron-proton interaction restores the N=20 shell gap when the valley of stability is approached
- Spin-Tensor decomposition shows it is mainly a Central and Tensor effect

Island of Inversion: Trends

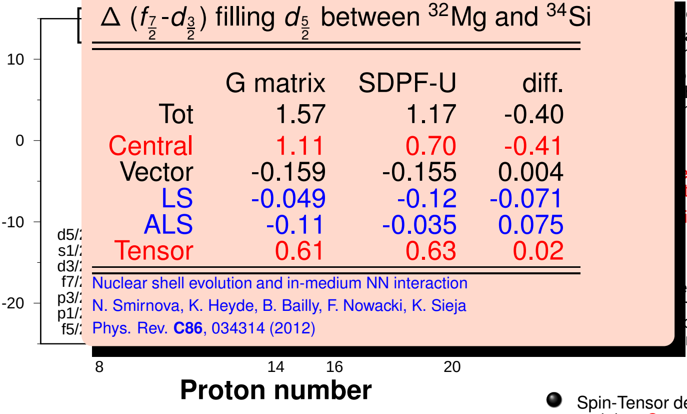

$\Delta\ (f_{\frac{7}{2}}\text{-}d_{\frac{3}{2}})$ filling $d_{\frac{5}{2}}$ between ^{32}Mg and ^{34}Si

	G matrix	SDPF-U	diff.
Tot	1.57	1.17	-0.40
Central	1.11	0.70	-0.41
Vector	-0.159	-0.155	0.004
LS	-0.049	-0.12	-0.071
ALS	-0.11	-0.035	0.075
Tensor	0.61	0.63	0.02

Nuclear shell evolution and in-medium NN interaction
N. Smirnova, K. Heyde, B. Bailly, F. Nowacki, K. Sieja
Phys. Rev. **C86**, 034314 (2012)

- ...n drip line, the ESPE's of ...etely at variance with ...at the stability valley. The ...he standard ESPE's of ...malous ones in ^{28}O is ...he interactions of *sd* shell ...ng themselves
- ...*sd* shell orbits remain ...th *pf* shell with the $\nu 0f_{\frac{7}{2}}$ ...itals DO get inverted
- ...part of the ...interaction restores the ...when the valley of ...roached
- Spin-Tensor decomposition shows it is mainly a Central and Tensor effect

Island of Inversion: Trends

$\Delta\ (f_{\frac{7}{2}}\text{-}d_{\frac{3}{2}})$ filling $d_{\frac{5}{2}}$ between ^{32}Mg and ^{34}Si

	G matrix	SDPF-U	diff.
Tot	1.57	1.17	-0.40
Central	1.11	0.70	-0.41
Vector	-0.159	-0.155	0.004
LS	-0.049	-0.12	-0.071
ALS	-0.11	-0.035	0.075
Tensor	0.61	0.63	0.02

Nuclear shell evolution and in-medium NN interaction
N. Smirnova, K. Heyde, B. Bailly, F. Nowacki, K. Sieja
Phys. Rev. **C86**, 034314 (2012)

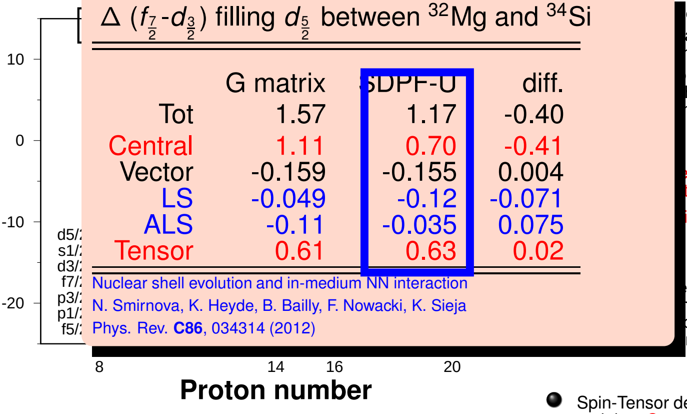

- At the neutron drip line, the ESPE's of ...etely at variance with ...at the stability valley. The ...he standard ESPE's of ...malous ones in ^{28}O is ...he interactions of *sd* shell ...ng themselves

...*sd* shell orbits remain ...th *pf* shell with the $\nu 0f_{\frac{7}{2}}$ ...itals DO get inverted

...part of the ...interaction restores the ...o when the valley of ...roached

- Spin-Tensor decomposition shows it is mainly a Central and Tensor effect

Correlation Energies

- Let us consider the configurations with closed N=20 $[sd]^{12,Z}$ (normal filling) and the ones with two neutrons blocked in the *pf* shell $[sd]^{10,Z}[pf]^{2,0}$ (intruder)

- And calculate the energy of the ground states at fixed configuration, with and without correlations

Correlations energies: normal vs 2p-2h intruder

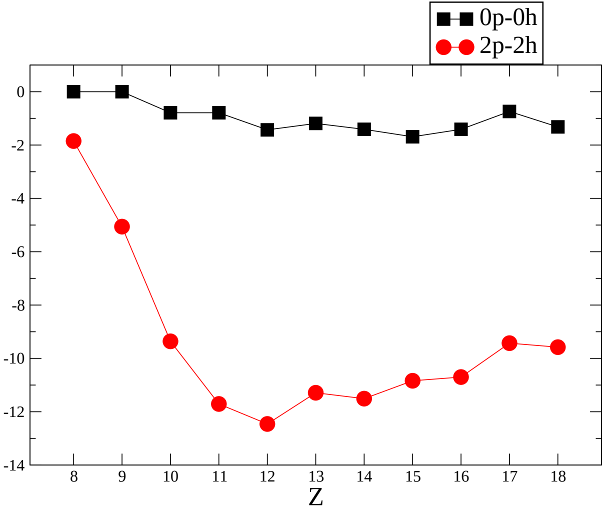

Gaps: normal vs 2p-2h intruder

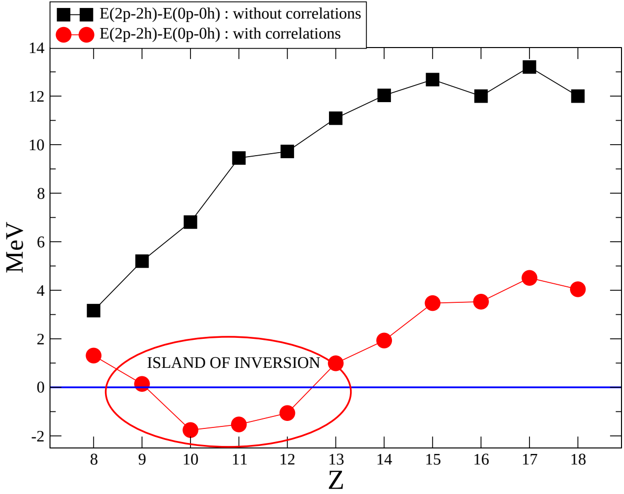

ESPE's vs Correlation Energies

- it is evident that the occurence of the "island of inversion" depends on subtle cancellations between monopole losses and correlations gains by the intruder states

- Notice that the correlations energies can be huge. For instance, in ^{32}Mg, the correlation energy of the lowest 0^{+} state in the 0p-0h, 2p-2h and 4p-4h configurations is respectively, 1.5 MeV (spherical), 12.5 MeV (deformed) and 21 MeV !!! (superdeformed)

Spherical, Deformed and Superdeformed states in ^{32}Mg

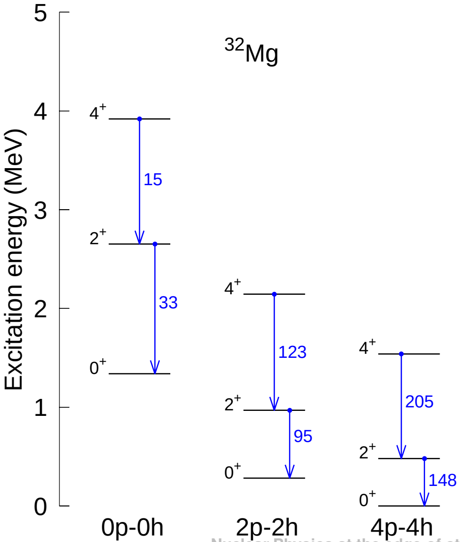

Quadrupole Collectivity vs Magic Closures N=20

- Four protons away from doubly magic ^{40}Ca, ^{34}Si is a new doubly magic nucleus because the normal filling configuration dominates the ground state with the deformed 2p-2h being the first excited state at 2.7 MeV. The first excited 2^+ at 3.33 MeV is also of 2p-2h nature
- To go even more neutron rich, one needs to remove protons from the $0d_{\frac{5}{2}}$ orbit
- This causes a small reduction of the N=20 neutron gap, and an increase of the correlation energy of the intruder which is enough to make it the ground state
- In this way we suddenly land in the Island of Inversion in which Deformed Intruder states become ground states, as in ^{32}Mg, ^{31}Na and ^{30}Ne

Inverse shape coexistence Shell closure in ^{32}Mg

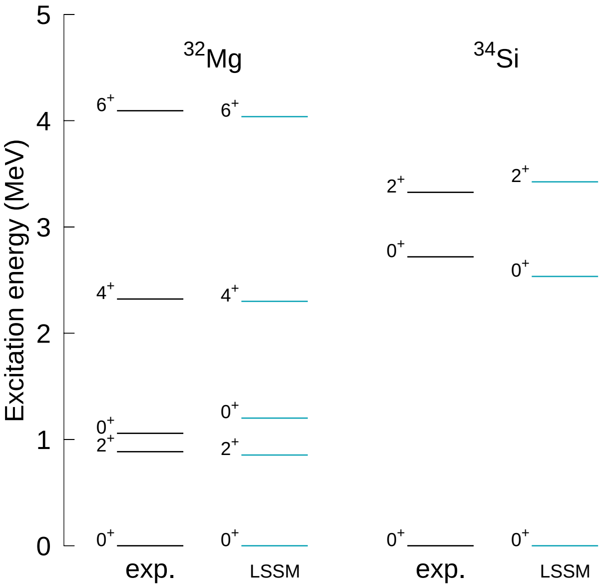

The structure of the 0^+ states: coexistence

- ^{30}Mg
  - 0^+_{gs} 0p-0h 77% . . . 2p-2h (ND) 22%
  - 0^+_{ex} 0p-0h 18% . . . 2p-2h (ND) 77%
- ^{32}Mg
  - 0^+_{gs} 0p-0h 12% . . . 2p-2h (ND) 56% . . . 4p-4h (SD) 31%
  - 0^+_{ex} 0p-0h 42% . . . 2p-2h (ND) 08% . . . 4p-4h (SD) 50%
- ^{34}Mg
  - 0^+_{gs} 0p-0h 89% . . . 2p-2h (ND) 11%
  - 0^+_{ex} 0p-0h 06% . . . 2p-2h (ND) 87%

Silicium and Magnesium chains

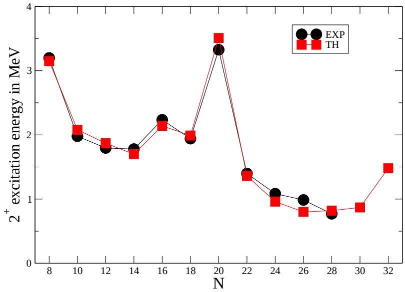

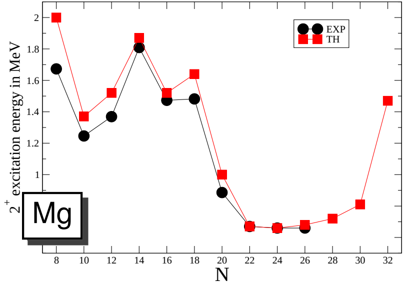

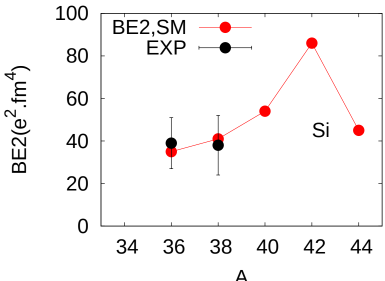

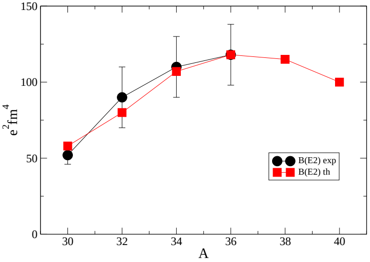

Further away from Stability

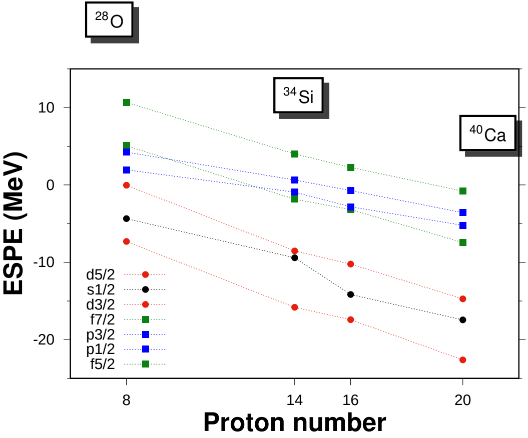

- At the neutron drip line, the ESPE's of ^{28}O are completely at variance with those of ^{40}Ca at the stability valley. The change from the standard ESPE's of ^{16}O to the anomalous ones in ^{28}O is totally due to the interactions of *sd* shell neutrons among themselves
- Notice that the *sd* shell orbits remain always below th *pf* shell with the $\nu 0f_{\frac{7}{2}}$ and $\nu 0p_{\frac{3}{2}}$ orbitals DO get inverted
- The monopole part of the neutron-proton interaction restores the N=20 shell gap when the valley of stability is approached
- Shell Evolution favors natural geometry for low-lying M1 excitations

$$\begin{matrix} \nu 1s_{\frac{1}{2}} \\ \nu 0d_{\frac{3}{2}} \end{matrix} \otimes \begin{matrix} \nu 1p_{\frac{3}{2}} \\ \nu 1p_{\frac{1}{2}} \end{matrix}$$

Further away from Stability

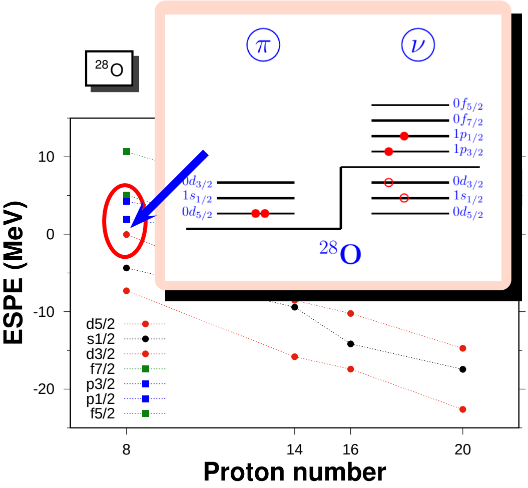

- At the neutron drip line, the ESPE's of ^{28}O are completely at variance with those of ^{40}Ca at the stability valley. The change from the standard ESPE's of ^{16}O to the anomalous ones in ^{28}O is totally due to the interactions of *sd* shell neutrons among themselves
- Notice that the *sd* shell orbits remain always below th *pf* shell with the $\nu 0f_{\frac{7}{2}}$ and $\nu 0p_{\frac{3}{2}}$ orbitals DO get inverted
- The monopole part of the neutron-proton interaction restores the N=20 shell gap when the valley of stability is approached
- Shell Evolution favors natural geometry for low-lying M1 excitations

$$\begin{matrix} \nu 1s_{\frac{1}{2}} \\ \nu 0d_{\frac{3}{2}} \end{matrix} \otimes \begin{matrix} \nu 1p_{\frac{3}{2}} \\ \nu 1p_{\frac{1}{2}} \end{matrix}$$

Neon chain

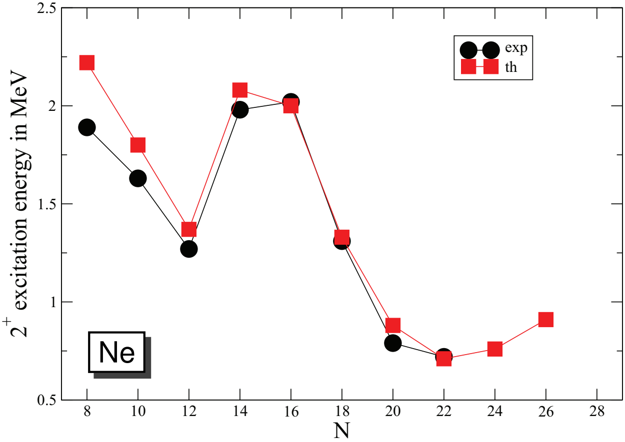

- Neons isotopes behave like magnesium isotopes

E1 strength in even neon isotopes

- SM in *psdpf* model space
- full *sd* diagonalization + full $1\hbar\omega$ excitations
- Exact removal of COM components

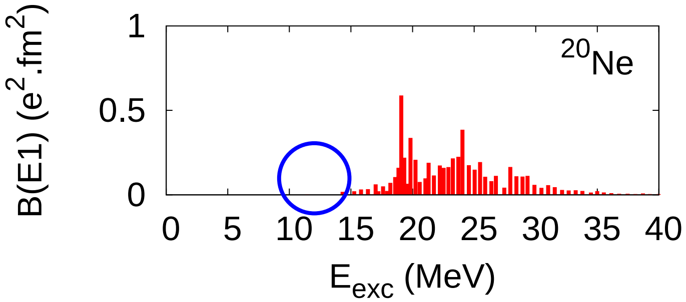

E1 strength in even neon isotopes

- SM in *psdpf* model space
- full *sd* diagonalization + full 1$\hbar\omega$ excitations
- Exact removal of COM components

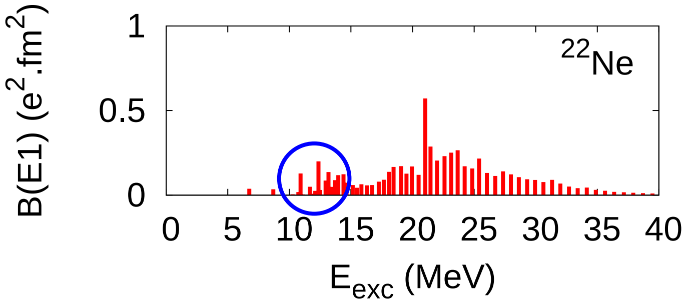

E1 strength in even neon isotopes

- SM in *psdpf* model space
- full *sd* diagonalization + full $1\hbar\omega$ excitations
- Exact removal of COM components

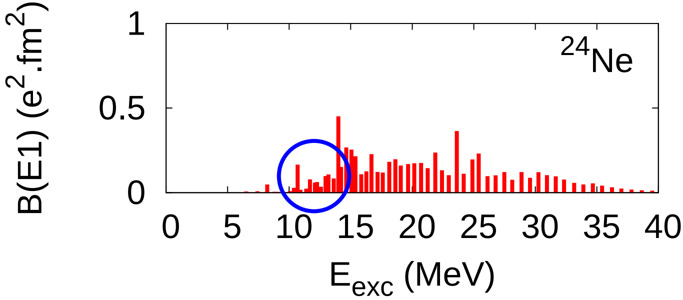

E1 strength in even neon isotopes

- SM in *psdpf* model space
- full *sd* diagonalization + full $1\hbar\omega$ excitations
- Exact removal of COM components

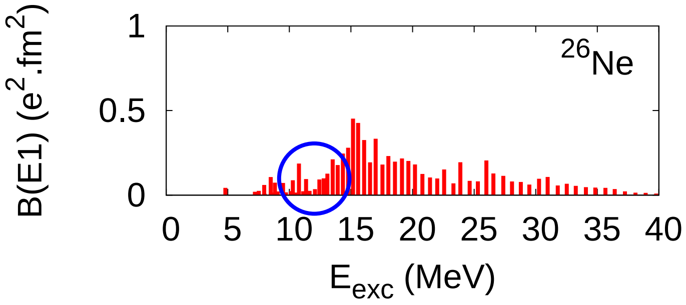

The case of ^{26}Ne

EXP: $\sum$B(E1)=0.49 $\pm$ 0.16 e^{2}fm^2 (6-10MeV)

THEO: $\sum$ B(E1)=0.485 e^{2}fm^2 (0-10MeV)

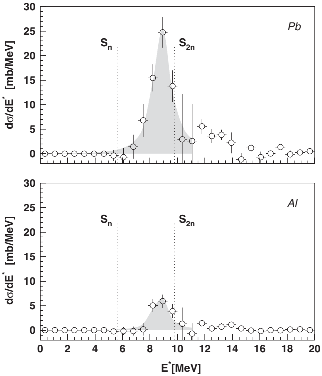

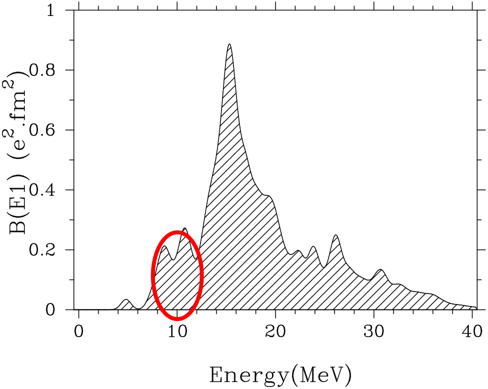

J. Gibelin et al., Phys. Rev. Lett. 101 (2008) 212503

Complex wave function

Major contribution from $\nu s^{-1}_{1/2}p^{1}_{3/2}$, $\nu s^{-1}_{1/2}p^{1}_{1/2}$ in agreement with QRPA results

M. Martini, S. Péru, and M. Dupuis, Phys. Rev. C 83, 034309 (2011)

E1 strength in even neon isotopes

- SM in *psdpf* model space
- full *sd* diagonalization + full $1\hbar\omega$ excitations
- Exact removal of COM components

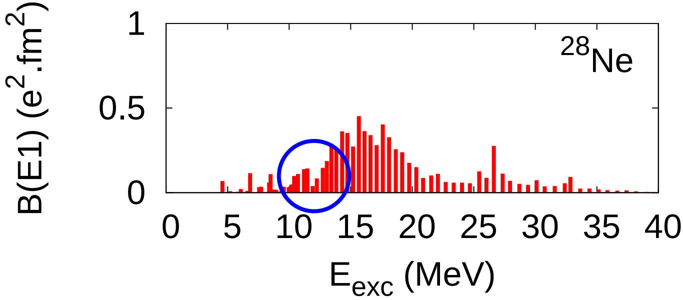

E1 strength in even neon isotopes

- SM in *sd-pf* model space
- t=4 *sd-pf* diagonalization for GS + 1p1h
- COM spuriosity $\sim$ 1%

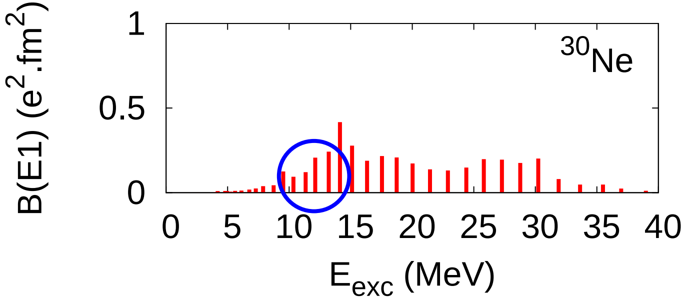

E1 strength in even neon isotopes

- SM in *sd-pf* model space
- t=4 *sd-pf* diagonalization for GS + 1p1h
- COM spuriosity $\sim$ 1%

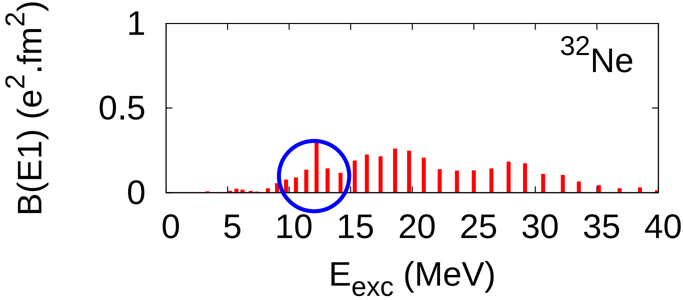

Evolution of dipole strength along the Ne chain

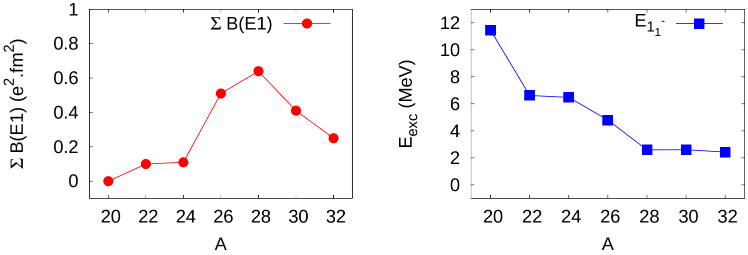

- The low lying strength moves up in energy in the island of inversion

nn interaction: Oxygen masses

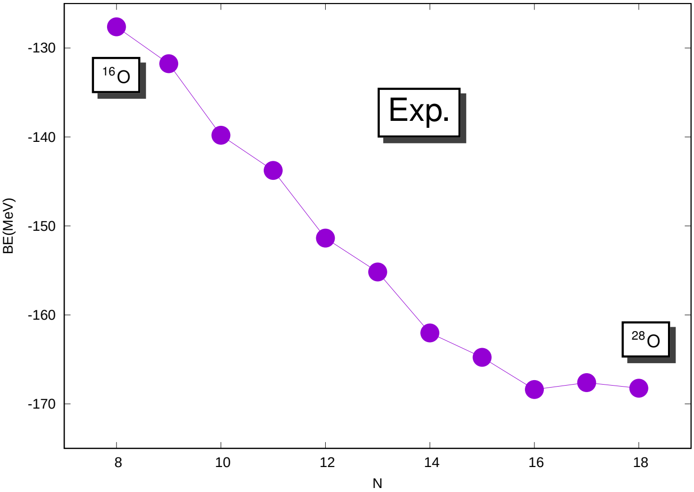

nn interaction: Oxygen masses

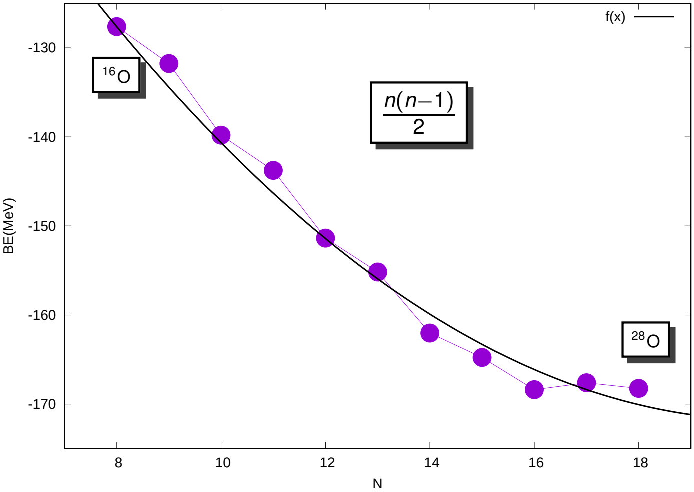

nn interaction: Oxygen masses

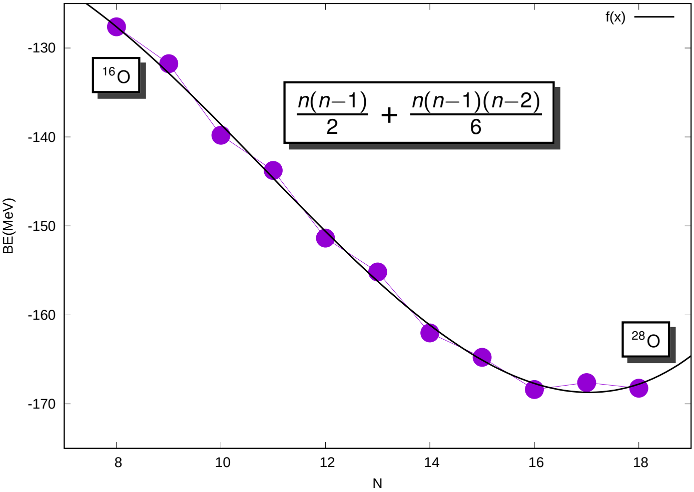

nn interaction: Oxygen masses

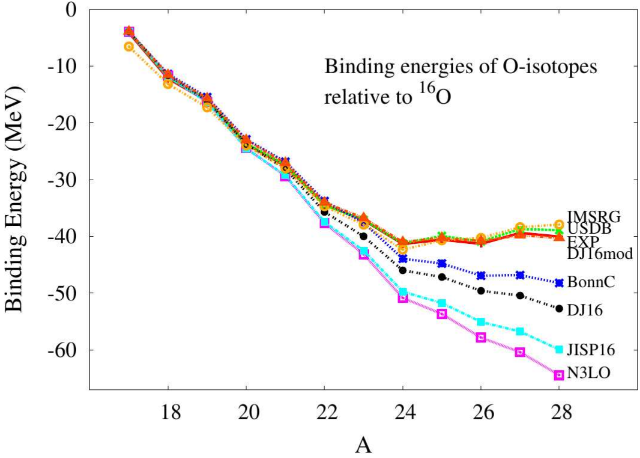

Microscopic sd-shell interactions from NCSM
N. Smirnova, B. R. Barrett et al.

RESANET GT3 meeting, Saclay 13/11/2018

RAPID COMMUNICATIONS

PHYSICAL REVIEW C **85**, 011302(R) (2012)

Low-lying neutron fp-shell intruder states in ^{27}Ne

S. M. Brown,[1] W. N. Catford,[1] J. S. Thomas,[1] B. Fernández-Domínguez,[2,3] N. A. Orr,[2] M. Labiche,[4] M. Rejmund,[5] N. L. Achouri,[2] H. Al Falou,[2] N. I. Ashwood,[6] D. Beaumel,[7] Y. Blumenfeld,[7] B. A. Brown,[8] R. Chapman,[9] M. Chartier,[3] N. Curtis,[6] G. de France,[5] N. de Sereville,[7] F. Delaunay,[2] A. Drouart,[10] C. Force,[5] S. Franchoo,[7] J. Guillot,[7] P. Haigh,[6] F. Hammache,[7] V. Lapoux,[10] R. C. Lemmon,[4] A. Leprince,[2] F. Maréchal,[7] X. Mougeot,[10] B. Mouginot,[7] L. Nalpas,[10] A. Navin,[5] N. P. Patterson,[1] B. Pietras,[3] E. C. Pollacco,[10] A. Ramus,[7] J. A. Scarpaci,[7] I. Stefan,[7] and G. L. Wilson[1]

LOW-LYING NEUTRON fp-SHELL INTRUDER STATES . . .

TABLE I. Comparison between experimental and calculated (see text) excitation energies and spectroscopic factors for states in ^{27}Ne. Experimental excitation energies are from [10] except for the 1.74-MeV state (present work). For C^2S, the errors include uncertainties from the reaction model.

J^π	E^*_{exp} (MeV)	$E^*_{WBP\text{-}M}$ (MeV)	C^2S Ref. [10]	C^2S Present	C^2S WBP-M
$3/2^+$	0	0	0.2(2)	0.42(22)	0.63
$3/2^-$	0.765	0.809	0.6(2)	0.64(33)	0.67
$1/2^+$	0.885	0.869	0.3(1)	0.17(14)	0.17
$7/2^-$	1.74	1.686	–	0.35(10)	0.40

At the neutron drip line, the ESPE's of ^{28}O are completely at variance with those of ^{40}Ca at the stability valley. The change from the standard ESPE's of ^{16}O to the anomalous ones in ^{28}O is totally due to the interactions of *sd* shell neutrons among themselves

- Notice that the *sd* shell orbits remain always below th *pf* shell with the $\nu 0f_{\frac{7}{2}}$ and $\nu 0p_{\frac{3}{2}}$ orbitals DO get inverted
- The monopole part of the neutron-proton interaction restores the N=20 shell gap when the valley of stability is approached
- Evidence for shell inversion towards ^{28}O

At the drip line

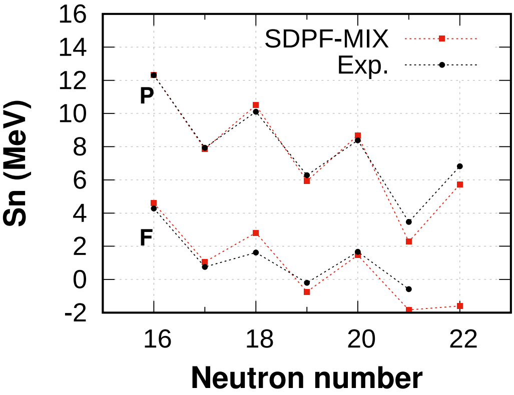

Nowacki/Poves 2014

- At the neutron drip line, the ESPE's of ^{28}O are completely at variance with those of ^{40}Ca at the stability valley. The change from the standard ESPE's of ^{16}O to the anomalous ones in ^{28}O is totally due to the interactions of *sd* shell neutrons among themselves
- Notice that the *sd* shell orbits remain always below th *pf* shell with the $\nu 0f_{\frac{7}{2}}$ and $\nu 0p_{\frac{3}{2}}$ orbitals DO get inverted
- The monopole part of the neutron-proton interaction restores the N=20 shell gap when the valley of stability is approached
- "ill" behaviour mainly due to ^{38}P separation energy

At the drip line

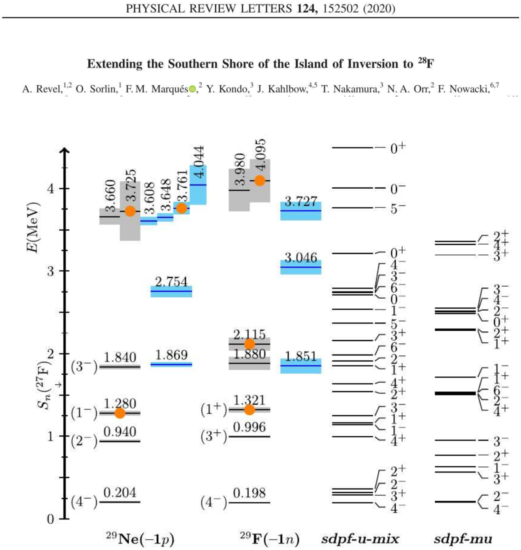

- At the neutron drip line, the ESPE's of ^{28}O are completely at variance with those of ^{40}Ca at the stability valley.
- Notice that the *sd* shell orbits remain always below th *pf* shell with the $\nu 0f_{\frac{7}{2}}$ and $\nu 0p_{\frac{3}{2}}$ orbitals DO get inverted
- Recent evidence for intruder states in ^{28}F low-lying spectrum
- In addition, extraction of 80% of "l=1" content in the GS

At the drip line

Continuum-coupling correction to binding

$$E_{corr;i}(E) = \mathrm{Re}\left\{\left\langle \Psi_i^A \middle| \mathcal{H}_{QQ}^{eff}(E) - H_{QQ} \middle| \Psi_i^A \right\rangle\right\}$$

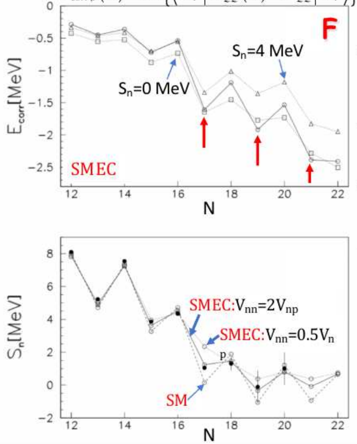

- Anti-odd-even staggering of continuum coupling energy correction E_{corr}
- $\langle \Phi_{g.s.}^{A-2} | [a_\nu a_\nu]^{J=0} | \Phi_{g.s.}^{A} \rangle$ in SM and SMEC are similar
- Blocking mechanism gradually disappears and Δ(N)→const(N)
- Reduction of the continuum coupling strength V_{np} if $S_n \gg S_p$ ($S_n \ll S_p$)

Y. Luo et al., arXiv:nucl-th/0211068

Y. Luo, J. Okolowicz, M.Płoszajczak, N. Michel, arXiv:nucl-th/0211068

E's of
ith
ey. The
's of
O is
sd shell
main
$\nu 0 f_{\frac{7}{2}}$
ed
es the
of

At the drip line

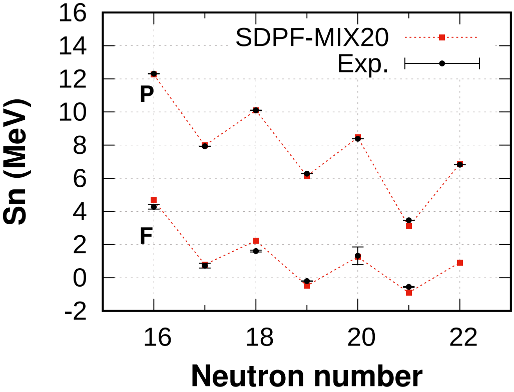

Nowacki/Poves 2020

- At the neutron drip line, the ESPE's of ^{28}O are completely at variance with those of ^{40}Ca at the stability valley. The change from the standard ESPE's of ^{16}O to the anomalous ones in ^{28}O is totally due to the interactions of *sd* shell neutrons among themselves
- Notice that the *sd* shell orbits remain always below th *pf* shell with the $\nu 0 f_{\frac{7}{2}}$ and $\nu 0 p_{\frac{3}{2}}$ orbitals DO get inverted
- The monopole part of the neutron-proton interaction restores the N=20 shell gap when the valley of stability is approached
- **New ^{30}F data from NeuLAND-SAMOURAI collaboration (J. Kahlbow phD work)**
- ^{38}P separation energy + $p_{3/2}$-$f_{7/2}$ splitting matches Fluorine chain S_n trend

At the drip line

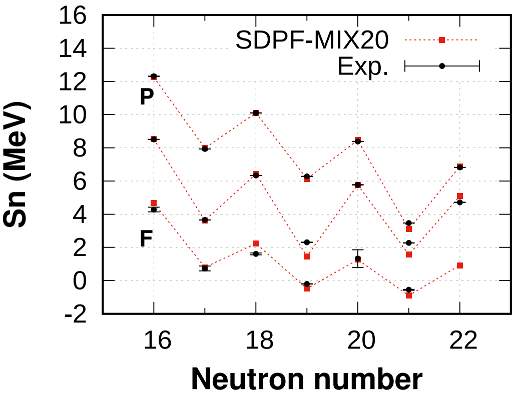

Nowacki/Poves 2020

- At the neutron drip line, the ESPE's of ^{28}O are completely at variance with those of ^{40}Ca at the stability valley. The change from the standard ESPE's of ^{16}O to the anomalous ones in ^{28}O is totally due to the interactions of *sd* shell neutrons among themselves
- Notice that the *sd* shell orbits remain always below th *pf* shell with the $\nu 0f_{\frac{7}{2}}$ and $\nu 0p_{\frac{3}{2}}$ orbitals DO get inverted
- The monopole part of the neutron-proton interaction restores the N=20 shell gap when the valley of stability is approached
- **New ^{30}F data from NeuLAND-SAMOURAI collaboration (J. Kahlbow phD work)**
- ^{38}P separation energy + $p_{3/2}$-$f_{7/2}$ splitting matches Fluorine chain S_n trend

At the drip line

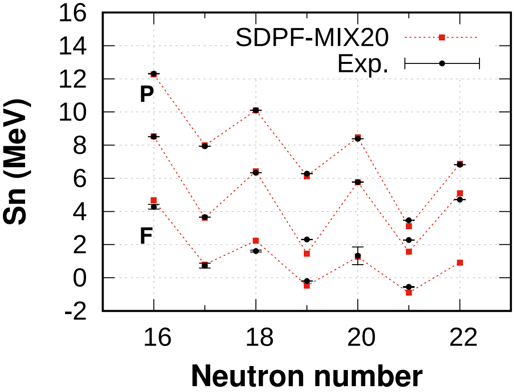

Nowacki/Poves 2020

- At the neutron drip line, the ESPE's of ^{28}O are completely at variance with those of ^{40}Ca at the stability valley. The change from the standard ESPE's of ^{16}O to the anomalous ones in ^{28}O is totally due to the interactions of *sd* shell neutrons among themselves
- Notice that the *sd* shell orbits remain always below th *pf* shell with the $\nu 0f_{\frac{7}{2}}$ and $\nu 0p_{\frac{3}{2}}$ orbitals DO get inverted
- The monopole part of the neutron-proton interaction restores the N=20 shell gap when the valley of stability is approached
- **New ^{30}F data from NeuLAND-SAMOURAI collaboration (J. Kahlbow phD work)**
- ^{38}P separation energy + $p_{3/2}$-$f_{7/2}$ splitting matches Fluorine chain S_n trend

At the drip line

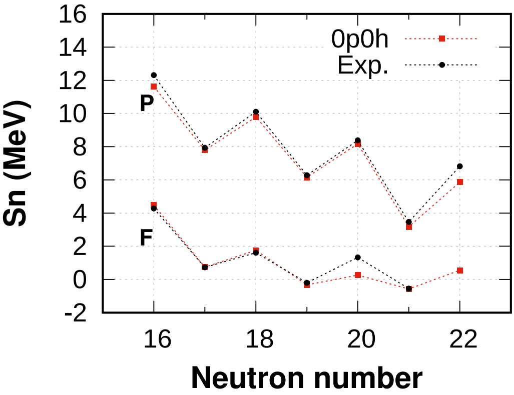

Core excitations effects

- At the neutron drip line, the ESPE's of ^{28}O are completely at variance with those of ^{40}Ca at the stability valley. The change from the standard ESPE's of ^{16}O to the anomalous ones in ^{28}O is totally due to the interactions of *sd* shell neutrons among themselves
- Notice that the *sd* shell orbits remain always below th *pf* shell with the $\nu 0 f_{\frac{7}{2}}$ and $\nu 0 p_{\frac{3}{2}}$ orbitals DO get inverted
- The monopole part of the neutron-proton interaction restores the N=20 shell gap when the valley of stability is approached
- ^{38}P separation energy + $p_{3/2}$-$f_{7/2}$ splitting matches Fluorine chain S_n trend

At the drip line

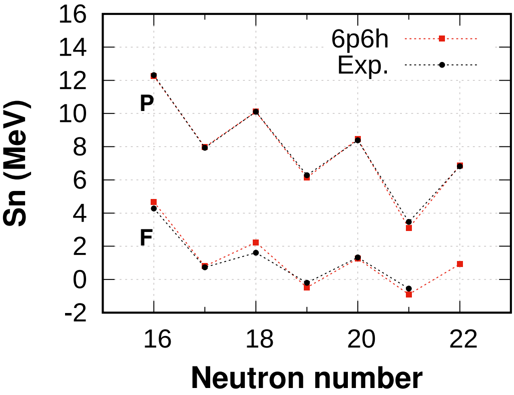

Core excitations effects

- At the neutron drip line, the ESPE's of ^{28}O are completely at variance with those of ^{40}Ca at the stability valley. The change from the standard ESPE's of ^{16}O to the anomalous ones in ^{28}O is totally due to the interactions of *sd* shell neutrons among themselves
- Notice that the *sd* shell orbits remain always below th *pf* shell with the $\nu 0f_{\frac{7}{2}}$ and $\nu 0p_{\frac{3}{2}}$ orbitals DO get inverted
- The monopole part of the neutron-proton interaction restores the N=20 shell gap when the valley of stability is approached
- ^{38}P separation energy + $p_{3/2}$-$f_{7/2}$ splitting matches Fluorine chain S_n trend

At the drip line

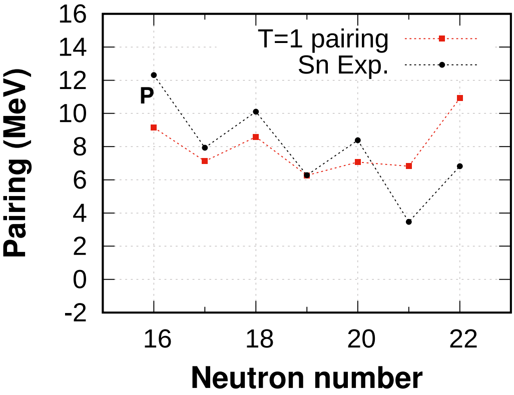

Pairing effects

- Stronger pairing correlations closer to Z=8 shell closure
- In ^{28}O, GS is dominated by 97% $v = 0$ components and more than 50% sd-pf n-n excitations. This pair scattering regime also appears in real continuum coupling (see Witek's talk and K. Fossez et al. PRC 96, 024308 (2017))
- In ^{29}F, GS is dominated by 70% $v = 0$ components and more than 60% sd-pf n-n excitations

At the drip line

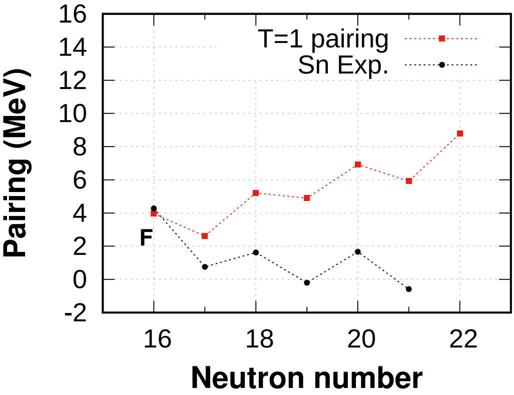

Pairing effects

- Stronger pairing correlations closer to Z=8 shell closure
- In ^{28}O, GS is dominated by 97% $v = 0$ components and more than 50% sd-pf n-n excitations. This pair scattering regime also appears in real continuum coupling (see Witek's talk and K. Fossez et al. PRC 96, 024308 (2017)
- In ^{29}F, GS is dominated by 70% $v = 0$ components and more than 60% sd-pf n-n excitations

At the drip line

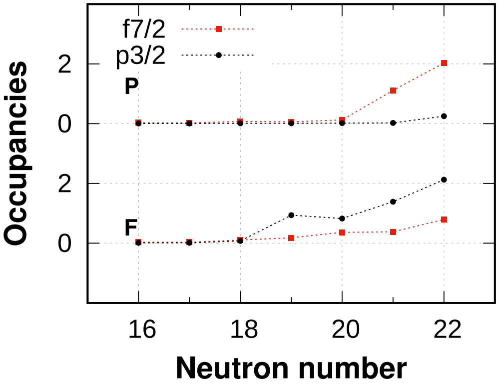

Occupancies effects

- Stronger pairing correlations closer to Z=8 shell closure
- In ^{28}O, GS is dominated by 97% $v = 0$ components and more than 50% sd-pf n-n excitations. This pair scattering regime also appears in real continuum coupling (see Witek's talk and K. Fossez et al. PRC 96, 024308 (2017))
- In ^{29}F, GS is dominated by 70% $v = 0$ components and more than 60% sd-pf n-n excitations

Summary

- Monopole drift develops in all regions but the Interplay between correlations (pairing + quadrupole) and spherical mean-field (monopole field) determines the physics.
  It can vary from :
  - island of deformation at N=20 and N=40
  - deformation at Z=14, N=28 for ^{42}Si and shell weakening at Z=28, N=50 for ^{78}Ni

- The “islands of inversion” appear due to the effect of the correlations, hence they could also be called “islands of enhanced collectivity”. As quadrupole correlations are dominant in this region, most of thei inhabitants are deformed rotors. Shape transitions and coexistence show up everywhere

- Quadrupole energies can be huge and understood in terms of symmetries

Summary

- even at the drip in fluorine isotopes, bound approximation holds
- strong superfluid regime with pair scattering from sd to pf shells
- odd-even Sn energies staggering does not seem to originate from continuum coupling

Special thanks to:

- A. Poves, S. Lenzi, K. Sieja
- O. Sorlin, A. Obertelli